Performance Evaluation of OFDM and Impulse-Radio Ultra-Wideband over Fiber Distribution for In-Building Networks

Marta Beltrán, Maria Morant, Joaquin Perez, and Roberto Llorente
Valencia Nanophotonics Technology Center
Universidad Politécnica de Valencia
Camino de Vera s/n, 46022 Valencia, Spain
mbeltran@ntc.upv.es

Abstract— **This paper reports the compared performance of the two main ultra-wideband (UWB) implementations, OFDM-based (OFDM-UWB) and impulse-radio UWB, when transmitted over optical fiber for in-building communications employing external electro-optic modulation. Both UWB implementations providing similar spectral efficiency, 0.378 bit/s/Hz and 0.392 bit/s/Hz respectively, are analyzed when transmitted over 300 m of standard single mode fiber (SSMF) or multimode fiber (MMF) link. The experimental results indicate that OFDM-UWB transmission is feasible for optical launch power levels of 2 dBm for both SSMF and MMF distribution. The impulse-radio UWB implementation achieves error-free SSMF transmission from -4 dBm launched power. The experimental results indicate that successful MMF transmission can be only achieved for impulse-radio UWB at 3 dBm launched power level.**

Keywords- Ultra-wideband (UWB); UWB-over-fiber; OFDM-UWB; impulse–radio UWB; in-building communications

I. INTRODUCTION

Ultra-wideband (UWB) radio technology has been proposed as a solution for wideband communications in the overspent spectrum, and has been regulated by the Federal Communications Commission for indoor communications [1]. In current regulation, UWB service is allocated in the band from 3.1 to 10.6 GHz [1-3], and is defined as signals with 20% fractional bandwidth or, at least, 500 MHz bandwidth.

Two main UWB implementations are available nowadays. From one side, WiMedia-defined signals which are based on multi-band orthogonal frequency division multiplexing (MB-OFDM) modulation that has been adopted in the standard ECMA-368 [3]. OFDM signals are intrinsically multipath robust due to the low symbol rate used and the addition of a guard period in the time signal [4]. On the other side, impulse-radio technology employs short radio pulses, typically of hundreds of picoseconds. Impulse-radio UWB is able to provide high-speed communications, localization and ranging (sub-centimeter resolution) simultaneously. In addition, impulse-radio UWB enables adjusting the desired bandwidth. This is not possible with OFDM-UWB, which are constrained to individual 528 MHz sub-bands. Impulse-radio UWB is not channelized, thus simplifying the overall system management.

Both implementations were proposed in [5] for access networks such as fiber-to-the-home (FTTH) and further analyzed experimentally reaching up to 60 km which could be used for long haul applications. The growing interest in FTTH architectures resides in the fact that optical fiber is replacing copper in access networks to connect subscribers directly. Standard single-mode fibers (SSMF) are extensively used for long-distance transmission and access networks, while multimode fibers (MMF) are used for short-distance communications like in-building transmission. The large core diameter of MMF fibers (typically of 50 μm or 62.5 μm) offers better source to fiber coupling resulting in easier installation for in-building environments and cheaper transmitters than in SSMF case by reduced assembly costs [6-7].

In this paper, UWB is proposed for in-building communications, and the transmission of both main implementations MB-OFDM and impulse-radio providing similar spectral efficiency (around 0.38 bit/s/Hz) is analyzed over different media. The fibers considered in this study comprise SSMF and MMF of 50 μm core with a length in the range of indoor applications of 300 m. This distance covers most of the connections in office networks. For example, in 2002 a 10 Gbit/s Ethernet transmission over a distance of 300 m (10GBASE-SX) was reached for data communication systems, in particular for backbone connections [6].

Several studies have been reported on UWB transmission for in-building applications, e.g. offices or home environments, evaluating the transmission coefficients of the building materials [8] or UWB signals robustness over multipath [9].

This paper is divided in six sections. Section II describes the in-building scenarios of application of this work. Section III describes the common setup implemented for the evaluation of the transmission of both UWB implementations (OFDM and impulse-radio) over different optical media (SSMF and MMF). The experimental setup and results for OFDM-UWB signals distribution are presented and discussed in Section IV, and the same is done for impulse-radio UWB signals in Section V. Finally, in Section VI the main conclusions are drawn.

This work has been partly funded by the European Commission through the FP7 ICT 216785 UCELLS project. The work of M. Beltrán and M. Morant is supported by Spain MICINN under FPI grant BES-2006-12066 and FPU grant AP2007-01413, respectively. The kind support of BONE ("Building the Future Optical Network in Europe") Network of Excellence is also acknowledged.

II. IN-BUILDING UWB APPLICATION SCENARIOS

After the development of fiber architectures in the backbone and access networks, the next step consists in extending the broadband capacity offered by those networks (i.e. FTTH) into residential environments. The in-building network should provide both wired and wireless services, and should operate with a variety of standards, such as MB-OFDM UWB, impulse-radio UWB, 802.16e WiMAX, or 802.11x among others. This scenario is depicted on Fig. 1. This paper presents a combined performance evaluation of OFDM-UWB and impulse-radio UWB in-building distribution.

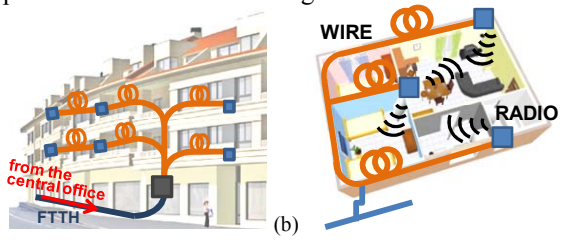

Figure 1. In-building scenarios for UWB radio-over-fiber distribution: (a) In-building network and (b) Distribution in office or home environments.

III. EXPERIMENTAL SET-UP

Fig. 2 shows the set-up implemented to evaluate the performance of the distribution of OFDM UWB and impulse-radio UWB over SSMF and MMF.

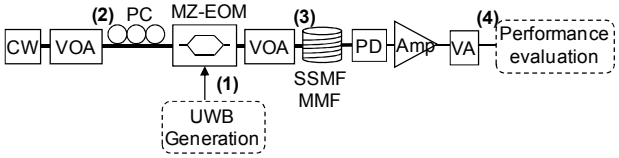

Figure 2. Experimental setup for performance evaluation of OFDM- and impulse-radio UWB distribution over fiber for indoor range. CW: Continuous-wave laser, VOA: Variable optical attenuator, PC: Polarization controller, PD: Photodetector, Amp: Electrical amplifier, VA: Variable electrical attenuator.

The UWB signal under study, whose generation is described in the next sections, is externally modulated with a continuous-wave optical carrier at 1555.75 nm by a Mach-Zehnder electro-optical modulator (MZ-EOM) (V_π=1.46 V_{DC}) working as a conventional double-sideband modulator. A variable optical attenuator is employed before the MZ-EOM to adjust the power launched to the fiber by adjusting the power at point (2) in Fig. 2 (from now referred as P2) emulating the central office as the incoming path shown in Fig. 1(a). The modulated signal is transmitted over fiber (SSMF or MMF) and the optical power launched to the fiber at point (3) in Fig. 2 (from now referred as P3) is adjusted with a second attenuator in order to analyze the link budget. After fiber transmission, the signal is photodetected properly depending on the optical media: A 40 GHz PIN photodiode is employed for SSMF and a 7 GHz photoreceiver consisting in a PIN photodiode with 50 µm MMF pigtail and an integrated transimpedance amplifier is employed for MMF transmission. Subsequently, the power spectral density (PSD) of the photodetected signal is adjusted with an electrical amplifier (26 dB gain and 5 dB noise figure) followed by a variable electrical attenuator to accomplish, at point (4) in Fig. 2, the UWB spectral mask defined in current regulation with a maximum PSD of -41.3 dBm/MHz [1-3].

Once the PSD is adjusted, the signal is demodulated and its performance is evaluated measuring quality parameters in each UWB implementation. Due to the different nature of the modulation of OFDM and impulse-radio signals, the measured quality parameters are different for each implementation. In the case of OFDM-UWB signals, the error vector magnitude (EVM) of the received constellation is measured for each frequency channel. The EVM is a figure of merit for assessing the quality of digitally modulated communication signals. The bit error rate (BER) is calculated from the EVM, as given by $BER = erfc(\sqrt{2}/EVM)$ [10] for a quadrature phase shift keying (QPSK) signal assuming Gaussian noise. The performance of OFDM-UWB signal in-building distribution is evaluated comparing with the ECMA-368 limit of 18.84% EVM [3], giving $3 \cdot 10^{-14}$ BER. In the case of impulse-radio UWB signals, the signal-to-noise ratio (Q-factor) is measured in the eye diagrams of the demodulated pulses. BER is then calculated from the Q-factor, as given by $BER = 0.5 \cdot erfc(Q/\sqrt{2})$, for equally probable data symbols assuming Gaussian noise. The performance of impulse-radio UWB signals in-building transmission is evaluated comparing with a typical system requirement for error-free transmission for BER of 10^{-9}. The BER limit is $2.2 \cdot 10^{-3}$ in case of incorporating forward error correction (FEC) codes.

IV. OFDM-UWB IN-BUILDING DISTRIBUTION

In order to evaluate the performance of OFDM-UWB in optical fiber in-building distribution, the measurement setup shown in Fig. 3 has been implemented according to Fig. 2. A multi-channel MB-OFDM UWB signal is generated combining the UWB signals from three transmitters (Wisair DV9110). Each UWB transmitter is located at frequency band #1, #2 and #3 respectively from UWB band group #1, performing a non-hopping time frequency code (TFC5, TFC6 and TFC7), which enables a multi-channel MB-OFDM UWB transmission. The OFDM signal comprises 3 channels of 528 MHz bearing 200 Mbit/s each with QPSK modulation (as specified in [3]). This provides an aggregated bitrate of 600 Mbit/s and 0.378 bit/s/Hz spectral efficiency (10 dB frequency range of 3.168-4.752 GHz). The maximum PSD of the generated OFDM-UWB signal is -42 dBm/MHz. The spectrum and constellations of the OFDM-UWB generated signal are shown in Fig. 4, which have been measured at point (1) in Fig. 3 by a digital sampling analyzer (DSA) (Agilent 80000B).

The EVM of the OFDM-UWB signal transmitted through fiber is measured by the DSA after PSD adjustment to -41.3 dBm/MHz maximum at point (4) in Fig. 3. EVM measurements are compared with the threshold imposed by ECMA-368 for MB-OFDM UWB successful communication [3]. BER is calculated for sake of comparison with the impulse-radio performance.

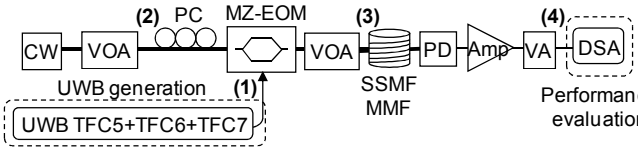

Figure 3. Experimental setup for OFDM-UWB distribution.

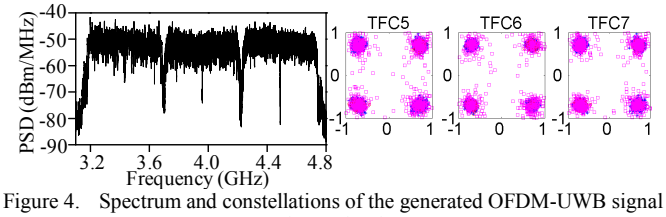

Figure 4. Spectrum and constellations of the generated OFDM-UWB signal at point (1) in Fig. 3.

In Fig. 5, EVM results and BER calculation for OFDM over 300 m SSMF transmission are presented and compared with optical back-to-back (B2B) configuration for the SSMF photodetector at a P2 of 13.9 dBm. These results indicate that successful SSMF transmission for the three OFDM channels simultaneously is achieved at a punctual P3 of 2 dBm. However, successful communication for the first UWB channel, TFC5, is achieved at P3 from 0 to 2 dBm while for the second UWB channel, TFC6, is achieved at P3 from 1 to 2 dBm. Comparing with B2B configuration, impairments due to SSMF distribution are similar for the three UWB channels.

Fig. 6 shows the MB-OFDM UWB spectrum and constellations for each channel received at DSA after 300 m SSMF fiber distribution. The frequency distortion is due to the frequency response of the attenuator employed to adjust the PSD at point (4) in Fig. 3. This causes worse EVM at higher frequencies in both B2B and SSMF transmission configurations. The EVM difference among channels is higher at lower P3 because the dynamic range is lower.

In Fig. 7, EVM results for OFDM-UWB over 300 m MMF 50 µm transmission are presented and compared with B2B configuration for the MMF photoreceiver at a P2 of 13.9 dBm.

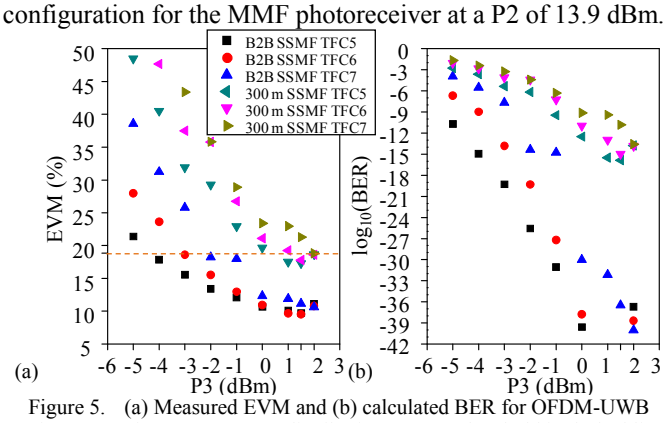

Figure 5. (a) Measured EVM and (b) calculated BER for OFDM-UWB performance after 300 m SSMF distribution. ECMA threshold in dashed line.

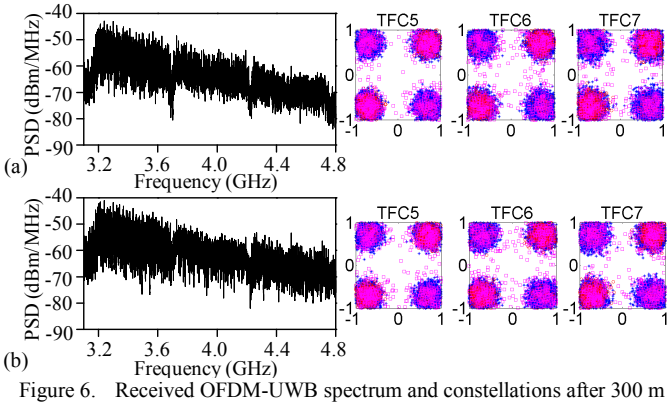

Figure 6. Received OFDM-UWB spectrum and constellations after 300 m SSMF distribution. (a) P3= 2 dBm. (b) P3= 1 dBm.

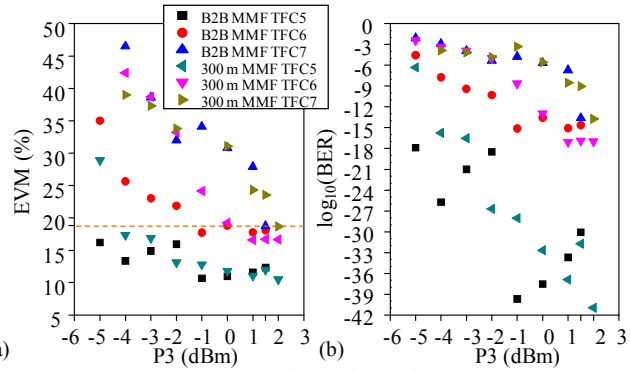

Figure 7. (a) Measured EVM and (b) calculated BER for OFDM-UWB performance after 300 m MMF distribution. ECMA threshold in dashed line.

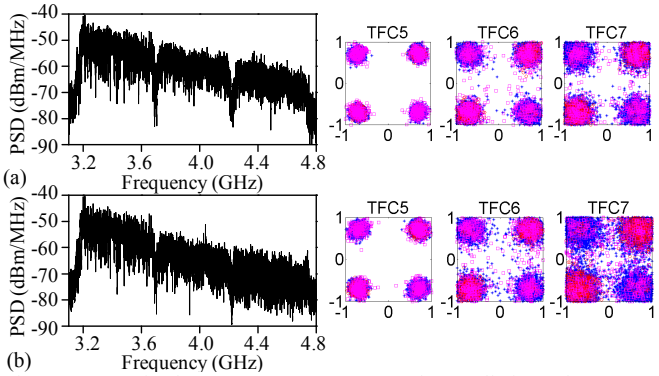

Figure 8. Received OFDM-UWB spectrum and constellations after 300 m MMF distribution. (a) P3= 2 dBm. (b) P3= 1 dBm.

The EVM results in Fig. 7 indicate that successful MMF transmission for the three OFDM channels simultaneously is achieved at 2 dBm. However, EVM for TFC5 UWB channel enables the successful MMF transmission at P3 from -4 to 2 dBm. Successful transmission of TFC6 channel is achieved at P3 from 0 to 2 dBm. Comparing with B2B configuration, impairments due to MMF distribution are different for the three UWB channels. MMF well-known transfer function introduces attenuation and distortion increasing with frequency due to the intermodal dispersion, which is noticeable in OFDM-UWB MMF distribution where TFC7 UWB channel has worse EVM results after MMF transmission than TFC5 UWB channel. Fig. 8 shows the UWB spectrum and constellations for each channel received at DSA after 300 m MMF fiber transmission.

Further measurements at P2 lower than 13.9 dBm leaded to worse EVM results. Also, EVM results are worse amplifying the generated OFDM-UWB signal at point (1) in Fig. 3.

V. Impulse-Radio UWB In-Building Distribution

The experimental setup implemented to evaluate the performance of impulse-radio UWB over fiber in-building distribution is shown in Fig. 9, according to Fig. 2.

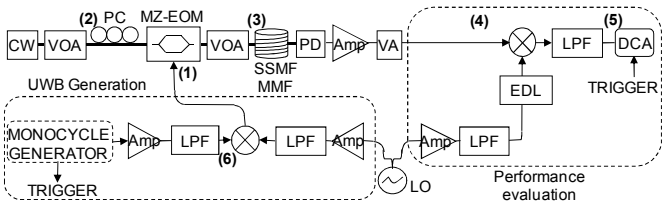

Figure 9. Experimental setup for impulse-radio UWB distribution. LPF: Low-pass filter, LO: Local oscillator, EDL: Electrical delay line.

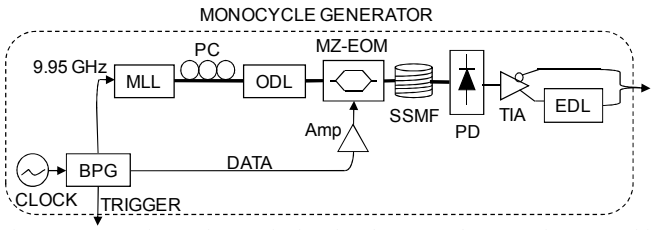

Figure 10. Experimental setup for baseband monocycle generation. BPG: bit pattern generator, MLL: Mode-locked laser, ODL: Optical delay line, TIA: Transimpedance amplifier, EDL: Electrical delay line.

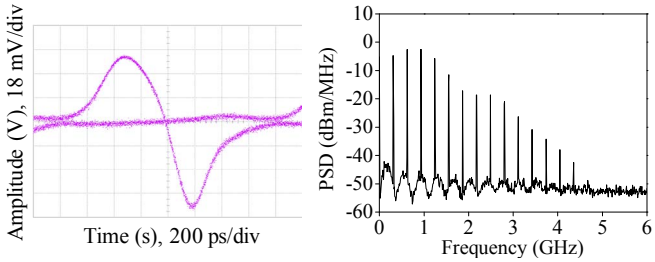

Figure 11. Baseband monocycle eye diagram and spectrum at Fig. 9 point (6).

First, baseband monocycles are generated as shown in Fig. 10 [11]. A return-to-zero data fixed sequence is generated at a bitrate of 622 Mbit/s. The modulation format employed is on-off keying (OOK) with ones and zeros equally frequent to emulate a random bit sequence. An actively mode-locked laser is employed to generate a high-quality optical pulse train at 1555.3 nm with 9.95 GHz repetition rate, 2 ps pulsewidth and 1.2 nm bandwidth (FWHM) which is intensity modulated with the data by a MZ-EOM. The data modulated optical pulses are time-stretched in 10 km of SSMF to adjust a suitable pulsewidth. Then, the stretched pulses are photodetected and amplified by a dual-output amplifier. The amplifier provides pulses of opposite polarity at the two outputs which are subsequently combined to shape monocycles. An electrical delay line is used at one amplifier output to adjust the relative delay between the two outputs. The photodetector and amplifier employed in the experiment are integrated in a dual photoreceiver with a limiting transimpedance amplifier (Teleoptix, DualPIN-DTLIA Rx) [12]. The pulsewidth, the pulse response of the photoreceiver, which is dependent on the threshold voltage controls of the limiting amplifier and the optical power applied to the photoreceiver, and the delay at the amplifier outputs are designed so that the generated monocycles exhibit approximately the same bandwidth as OFDM case, i.e. 1.584 GHz (3x528 MHz). The generated monocycles after amplification and low-pass filtering (3.3 GHz bandwidth) to remove noise are shown in Fig. 11. This signal corresponds to that measured at point (6) in Fig. 9.

Next, in order to meet the UWB mask in the same frequency range as OFDM case, the baseband monocycles are frequency up-converted by an electrical mixer. A local oscillator (LO) at 3.168 GHz with a power of 9 dBm (after amplification and 3.3 GHz low-pass filtering) is employed to perform the up-conversion. Thus, an impulse-radio UWB signal in approximately the same band as the three-channel OFDM signal employed in Section IV, as shown in Fig. 12(a), is generated at point (1) in Fig. 9. The impulse-radio UWB signal comprises a unique band in the 10 dB frequency range of approximately from 3.168 GHz to 4.752 GHz, bearing 622 Mbit/s and 0.392 bit/s/Hz spectral efficiency, similar to OFDM case for comparison purpose. The maximum PSD of the generated impulse-radio UWB signal is -23 dBm/MHz.

In practice, the impulse-radio UWB transmitted signal meeting the UWB mask, at point (4) in Fig. 9, has to be filtered to remove the undesired frequencies before being radiated. In the experiment, at receiver, this signal is directly demodulated by down-conversion employing an electrical mixer. The LO with a power of 7 dBm (after amplification and 3.3 GHz low-pass filtering) is employed to down-convert the impulse-radio UWB signal. An electrical delay line is used in the LO to fine tune the phase of the LO for accurate down-conversion. Afterwards, the down-converted signal is low-pass filtered (1.65 GHz bandwidth) and measured by a digital communications analyzer (DCA) (Agilent 86100C, HP83481A 12.4 GHz bandwidth). The Q-factor of the demodulated impulse-radio UWB signals is evaluated by the DCA in the measured eye diagrams.

Fig. 13 shows BER results for impulse-radio UWB over 300 m SSMF transmission and for the corresponding optical B2B configuration as a function of P2. The results indicate that error-free transmission is achieved in the range of P3 from -4 to 4.7 dBm; BER values maintain at P3 in the range from -3 to 2 dBm while the higher P3 the better BER at P3 higher than 2 dBm and the lower P3 the worse BER at P3 lower than -3 dBm; BER is independent on P2. Comparing to B2B case, the performance with SSMF transmission improves with respect to B2B at P3 in the range from -5 to 0 dBm. Note that at P3 lower than -5 dBm the -41.3 dBm/MHz PSD limit is not reached and higher P2 and/or PSD level at point (1) in Fig. 9 is required to adjust P3 higher than 4.7 dBm. Fig. 12(b) is an example of the spectrum at point (4) in Fig. 9 after 300 m SSMF. Fig. 14 shows the detected impulse-radio UWB pulses after 300 m SSMF distribution, measured at point (5) in Fig. 9.

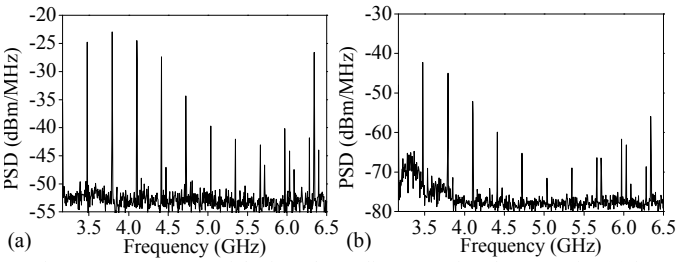

Figure 12. Spectrum of the impulse-radio UWB signal (a) at point (1) in Fig. 9, (b) at P2= 13.7 dBm and P3= -3 dBm at point (4) in Fig. 9.

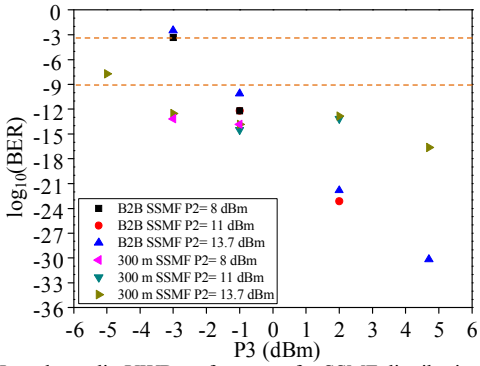

Figure 13. Impulse-radio UWB performance for SSMF distribution compared with optical back-to-back configuration. BER limits in dashed lines.

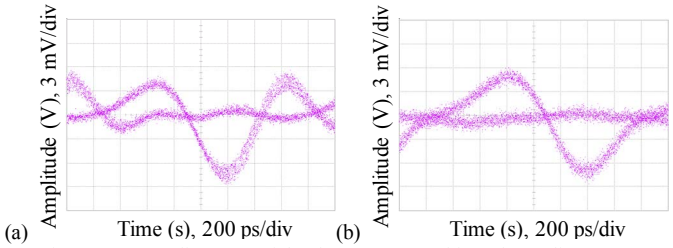

Figure 14. Eye diagrams of the down-converted impulse-radio UWB monocycles after 300 m SSMF distribution at point (5) in Fig. 9. (a) P2= 13.7 dBm, P3= 4.7 dBm. (b) P2= 13.7 dBm, P3= -3 dBm.

Fig. 15 shows BER results for impulse-radio UWB over 300 m MMF 50 µm transmission and for the corresponding B2B configuration as a function of P2. The results indicate that the best BER is achieved at P3 about 3 dBm for all P2 from 12 dBm to 13.7 dBm, but error-free transmission is only achieved at a P2 of 12 dBm. Comparing with B2B case, the performance with MMF transmission is always worse. Further observations are: No eye is measured in the range of P2 from 10.1 to 11.9 dBm and in the range of P3 from 2.5 to 2.9 dBm; There is an abrupt change in the eye at a P2 of 6.2 dBm and at P2 lower than 6.2 dBm the BER gets worse; From certain P3 between -1.8 dBm and 2.4 dBm there is an abrupt change in the eye at all P2 maintaining to lower values of P3, so that in the spectrum at point (4) in Fig. 9 spurious frequencies appearing are more significant, as shown in Fig. 16(b).

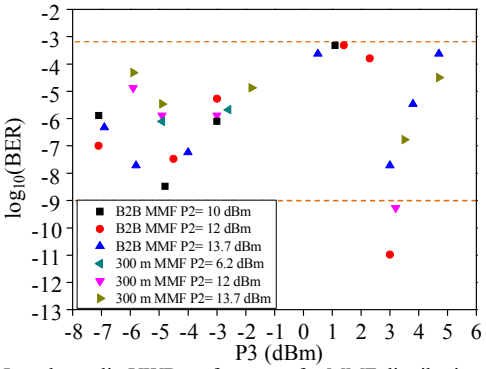

Figure 15. Impulse-radio UWB performance for MMF distribution compared with optical back-to-back configuration. BER limits in dashed lines.

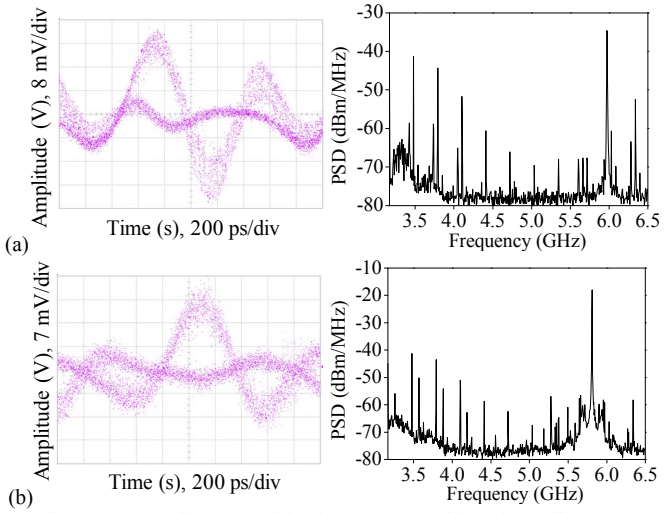

Figure 16. Eye diagrams of the down-converted impulse-radio UWB monocycles at point (5) in Fig. 9 after 300 m MMF and spectrums at point (4) in Fig. 9. (a) P2=12 dBm and P3=3.2 dBm.(b) P2=12 dBm and P3= -4.9 dBm.

Fig. 16 shows the spectrums and eye diagrams of the detected impulse-radio UWB pulses after 300 m MMF distribution, measured at point (5) in Fig. 9. The BER behavior as a function of P2 and P3 is ascribed mainly to the saturation of the amplifier in the photoreceiver.

Note that at other P2, P3 and/or PSD level at point (1) in Fig. 9, the BER behavior is the same as that in a certain zone shown in Fig. 15 but obtaining different BER values. Error-free transmission is not achieved at maximum PSD lower than -23 dBm/MHz at point (1) in Fig. 9.

VI. Conclusion

In conclusion, from the experimental results, impulse-radio UWB requires less optical launched power than its OFDM-UWB counterpart for successful SSMF transmission over a distance of 300 m. In the case of MMF, the experimental results exhibit a large variance and successful transmission over 300 m can only be achieved at a launched power of 2 dBm for complete OFDM-UWB or 3 dBm for impulse-radio UWB. We believe that this behavior is due to the saturation of the limiting amplifier integrated in the MMF photoreceiver and to the transfer function of the MMF.

Acknowledgment

The authors acknowledge Teleoptix, B.U. of Linkra s.r.l., Cornate d'Adda (MI) - Italy, for supplying the dual photoreceiver.

References

[1] FCC 02-48: “Revision of part 15 of the commission’s rules regarding ultra-wideband transmission systems,” April 2002.

[2] ECC/DEC/(06)04: “On the harmonised conditions for devices using ultra-wideband (UWB) technology in bands below 10.6 GHz,” March 2006.

[3] ECMA-368 International Standard: “High rate ultra wideband PHY and MAC standard,” Dec. 2008.

[4] D. Lee, and K. Cheun, “A new symbol timing recovery algorithm for OFDM systems,” IEEE Trans. Consum. Electron., vol. 43, no. 3, pp. 766-775, Aug. 1997.

[5] R. Llorente, et al., “Ultra-wideband radio signals distribution in FTTH networks,” IEEE Photonics Technology Letters, vol. 20, no. 11, pp. 945-947, June 2008.

[6] L-A de Montmorillon, G. Kuyt, P. Nouchi, and A. Bertaina, “Latest advances in optical fibers,” C. R. Physique 9, pp. 1045–1054, 2008.

[7] A.M.J. Koonen, and L.M. Garcia, “Radio-over-MMF techniques-Part II: Microwave to millimeter-wave systems,” IEEE Journal Lightwave Technology, vol. 26, no. 15, pp. 2396-2408, Aug. 2008.

[8] R-R. Lao, J-H. Tamg, and C. Hsiao, “Transmission coefficients measurement of building materials for UWB systems in 3-10 GHz,” IEEE Vehicular Technol. Conf. Spring 2003, pp. 11-14, April 2003.

[9] M. Z. Win, and R. A. Scholtz, “On the robustness of ultra-wide bandwidth signals in dense multipath environments,” IEEE Communications Letters, vol. 2, no. 2, Feb. 1998.

[10] R.A.Shafik, M.S. Rahman, and A.H.M.R. Islam, “On the extended relationships among EVM, BER and SNR as performance metrics,” International Conf. on Electrical and Computer Engineering, Dec. 2006.

[11] M. Beltrán, R. Llorente, R. Sambaraju, and J. Martí, “60 GHz UWB-over-fiber system for in-flight communications,” 2009 IEEE MTT-S Int. Microwave Symposium, pp. 5-8, June 2009.

[12] Teleoptix, 43 Gbit/s Balanced PHOTORECEIVER with limiting TIA (DualPIN-DTLIA Rx), http://www.teleoptix.com